

PHYSICS OF ULTRACOLD ATOMS AND THEIR APPLICATIONS https://doi.org/10.1070/QEL16733

Work on the physics of ultracold atoms in Russia

In December 2017, the regular All-Russian Conference 'Physics of Ultracold Atoms' was held. Several tens of Russian scientists from major scientific centres of the country, as well as a number of leading foreign scientists took part in the Conference. The Conference topics covered a wide range of urgent problems: quantum metrology, quantum gases, waves of matter, spectroscopy, quantum computing, and laser cooling. This issue of Quantum Electronics publishes the papers reported at the conference and selected for the Journal by the Organising committee.

N.N. Kolachevsky, A.V. Taichenachev

https://doi.org/10.1070/QEL16658

Crossover from an atomic Fermi gas to a molecular Bose gas in a 2D system

V.B. Makhalov, A.V. Turlapov

Abstract. **The results of experimental and theoretical studies of a smooth crossover from a kinematically 2D Fermi gas of ultracold atoms into a Bose gas of molecular dimers are compared. The main attention is paid to the measurements and calculations in the zero-temperature approximation. The discrepancies between the results are discussed along with the questions that remain still open.**

Keywords: *laser cooling, low temperatures, Bose–Einstein condensation, Fermi gas.*

Laser cooling and trapping of matter [1–3] are widely used in fundamental and applied research: standards of frequency and time have been created on the basis of ultracold atomic gases [4, 5]; the interference of de Broglie waves of atoms has made it possible to perform highly accurate measurements of angular and linear accelerations, including gravity acceleration [6]; gyroscopes based on ultracold atoms are being developed [7, 8]; the gas of ultracold atoms excited to Rydberg states [9, 10] is a promising medium for the implementation of quantum informatics algorithms [11].

In experiments with ultracold gases of Bose and Fermi atoms, a number of effects were first observed, the mathematical models of which form the basis of quantum physics, for example, the Fermi pressure [12] and Bose condensation [13]. To date, a wide range of experiments have been performed with Bose condensates [14–16] and Fermi gases [14, 17, 18].

V.B. Makhalov Institute of Applied Physics, Russian Academy of Sciences, ul. Ulyanova 46, 603950 Nizhny Novgorod, Russia; e-mail: vasiliy.makhalov@appl.sci-nnov.ru;
A.V. Turlapov Institute of Applied Physics, Russian Academy of Sciences, ul. Ulyanova 46, 603950 Nizhny Novgorod, Russia; N.I. Lobachevsky State University of Nizhny Novgorod, prosp. Gagarina 23, 603950 Nizhny Novgorod, Russia; e-mail: turlapov@appl.sci-nnov.ru

Received 21 February 2018; revised version 25 March 2018
Kvantovaya Elektronika **48** (5) 401–404 (2018)
Translated by M.A. Monastyrskiy

Rearranging the interactions by means of the Fano–Feshbach resonance [19] made it possible to adiabatically transform the gas of Fermi atoms into a Bose condensate of molecular dimers [14, 17]. From the theoretical viewpoint, a similar crossover was considered in the late 1960s for excitons [20] and electrons [21] and later for quarks [22], though only recently it was implemented in a gas of ultracold Fermi atoms [23] for 3D systems, and then for 2D ones [24].

Kinematically, 2D quantum systems attract attention due to the role of fluctuations, which increases with decreasing dimensionality. On the one hand, this complicates the description of such systems, and on the other hand, makes their physics more interesting [25, 26]. Two-dimensional fermion systems include an electron gas in layered systems, such as heterostructures [27] and high-temperature superconductors [28], ^{3}He films [29], and a so-called nuclear lasagne of neutron stars – a region with predominant 2D kinematics, which possibly limits the pulsar rotation period [30].

In this paper we discuss the results of studying the crossover between the fermion and boson states of a two-dimensional Fermi gas, that is, the crossover between the Bardeen–Cooper–Schrieiffer state and the Bose–Einstein condensate (BCS–BEC crossover). We consider a gas of Fermi atoms in two equally populated spin states interacting through *s*-wave scattering, the magnitude of which can continuously vary within the widest possible limits. The previously published experimental data and theoretical calculations are compared. The main attention is focused on measurements and calculations in the zero-temperature approximation. In experiments [24, 31, 32], measurements were conducted in an ultracold gas of Fermi atoms ^{6}Li trapped in a disk-like potential whose shape is close to parabolic:

$$V(\boldsymbol{x}) = \frac{m\omega_z^2 z^2}{2} + \frac{m\omega_\perp^2 (x^2 + y^2)}{2}, \qquad (1)$$

where m is the mass of atom; and ω_z and $\omega_\perp$ are the potential frequencies. The retention along the z axis is much 'stronger'

than that along other directions, i.e. $\omega_z \gg \omega_\perp$. Atoms or pairs of atoms mainly populate the ground state of motion along the z axis, which makes the system kinematically two-dimensional.

The pressure value is an indicator of the transition between the boson and fermion regimes. In the case when the total pressure of both spin components P is close to the pressure P_{ideal} of the ideal Fermi gas, the system is fermionic, while $P/P_{\text{ideal}} \ll 1$ corresponds to the bosonic regime. Note that $P_{\text{ideal}} = 2\pi n^2\hbar^2/m$, where n is the 2D concentration of each of the spin components, it also represents the concentration of molecules in the BEC limit; and the 2D pressure measurement units are the force divided by length.

The measured dependence of the normalised pressure P/P_{ideal} on the interaction parameter $a_2\sqrt{n}$, where a_2 is the 2D length of s-wave scattering, is shown in Fig. 1. Another alternative of the interaction parameter accepted in the literature is $k_F a_2$, where $k_F = \sqrt{4\pi n}$ is the Fermi wave vector. The relative pressure increase with increasing $a_2\sqrt{n}$ qualitatively corresponds to the picture of a crossover from the Bose gas of molecular dimers ($a_2\sqrt{n} \ll 1$) to the Fermi gas of atoms ($a_2\sqrt{n} \gg 1$). The pressure and concentration are measured at the centres of the disk-like clouds, because near the centre the gas state is closer to the state of a homogeneous gas and has the greatest degeneracy due to the smallest local value of T/ε_F, where T is the temperature, and $\varepsilon_F = 2\pi n\hbar^2/m$ is the Fermi energy. The dependence presented in Fig. 1 can be regarded as the equation of state of the gas, since the dependence relates the thermodynamic quantities P and n.

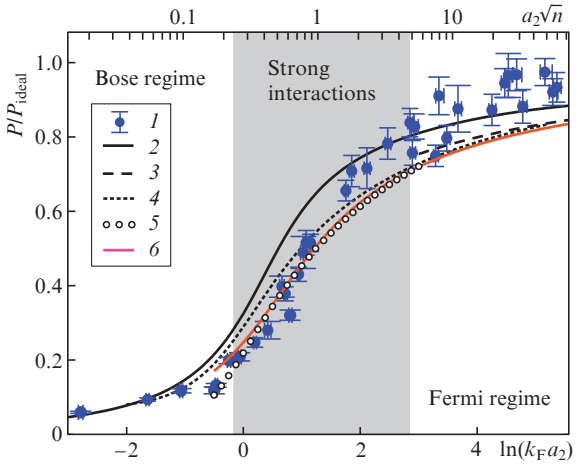

Figure 1. Normalised pressure at the cloud centre as a function of the interaction parameter: (*1*) data [24]; (*2*) mean-field approximation supplemented by fluctuations [33]; (*3*) Fermi-liquid theory [34]; (*4*) diffusion Monte Carlo method [35]; (*5*) Monte-Carlo method on the lattice [37]; (*6*) calculation using the Monte Carlo method with auxiliary fields [36].

The crossover between the fermion and bosonic regimes can also be observed from the change in the chemical potential μ, the results of the measurement of which are shown in Fig. 2; the designation ε_B corresponds to the binding energy of a diatomic molecule. In the zero-temperature approximation $dP = nd\mu$, which allows us to compare the data in Figs 1 and 2. Besides, we can compare the data with the calculations, the results of which are also presented in these Figures.

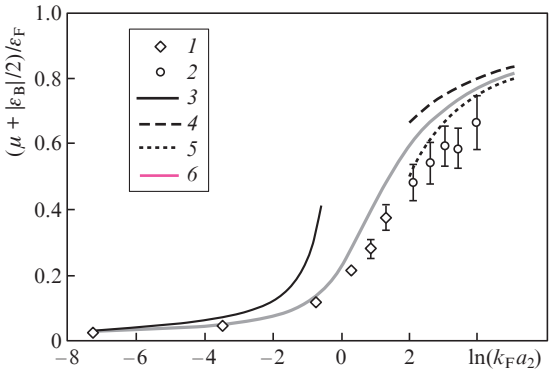

Figure 2. Low-temperature equation of state in the 2D BEC–BCS crossover. Experimental data [32] were obtained for a quasi-2D gas at the lowest attainable temperatures that correspond to $T/\varepsilon_F \simeq 0.05$ and 0.1 on the boson and fermion sides. Diamonds and circles are (*1*) superfluid and (*2*) normal phases; (*3*) mean-field formula $(\mu + |\varepsilon_B|/2)/\varepsilon_F = -1/[4\ln(k_F a_2)]$; (*4*, *5*) non-self-consistent $(1/[1 + \ln^{-1}(k_F a_2)])$ and self-consistent $(1 - \ln^{-1}(k_F a_2))$ calculations by the Hartree–Fock method for weakly attracting fermions; (*6*) state equation calculated for the ground state by the Monte Carlo method with additional fields [36] (reproduced with permission from [32], the rightholder is the American Physical Society, 2016).

We start the comparison from the fermion regime, $a_2\sqrt{n} \gg 1$, or (conditionally) $a_2\sqrt{n} > 5$, for which the expansion with respect to a small parameter is known. In the Fermi-liquid approximation [34], the pressure is given by expression

$$\frac{P}{P_{\text{ideal}}} = 1 + 2f_0 + (7 - 4\ln 2)f_0^2, \qquad (2)$$

where $f_0 = -1/[2\ln(k_F a_2)]$. This approximation is shown in Fig. 1 by curve (*3*). At $T = 0$, there should be an energy gap arising from pairing, which, however, does not significantly change the pressure due to gap smallness in the fermion regime and the pressure continuity in the course of phase transition.

In addition, for the data in Fig. 1, for $a_2\sqrt{n} \geqslant 5$ ($\ln(k_F a_2) \geqslant 2.9$), the gas is most likely in the regime of a Fermi liquid, since the temperature $T = (0.02–0.15)\varepsilon_F$ exceeds the pairing and phase transition temperature, which is $0.01\varepsilon_F$ at $a_2\sqrt{n} = 5$ and decreases with increasing $a_2\sqrt{n}$ [38]. For the data in Fig. 2, it was also noted (see [36]) that for $\ln(k_F a_2) > 2$ the gas is in a normal non-superfluid phase; the corresponding part of the data is plotted by circles. The Fermi-liquid equation of state (2) for $a_2\sqrt{n} \gg 1$ coincides with the calculation by the Monte Carlo method with auxiliary fields [36]. The latter calculation is shown by curves (*6*) in Figs 1 and 2 and serve as a benchmark for comparing the data on these Figures.

The data in Fig. 1 lie systematically above the curves calculated from the Fermi-liquid equation of state (2) or by the Monte Carlo method [36]. In the experiment [32], the opposite shift of the data is obvious: In the Fermi region, at $\ln(k_F a_2) > 2.9$, the data lie systematically below the Monte Carlo curve [36] and, therefore, systematically below the curve corresponding to the Fermi-liquid formula (2). Thus, the difference between the experimental data in Figs 1 and 2, obtained by different research teams in [24] and [32] respectively, is obvious. Therefore, if the corresponding pressure values would have been restored from the data in Fig. 2, they would be substantially lower than the data in Fig. 1. In these

experiments, a significantly different number of atoms were used, $\sim 10^3$ and $\sim 10^5$, respectively. It remains an open question whether the difference in the results of the two experiments is due to the difference in the number of particles or an experimental error. It should also be noted that the models for a homogeneous medium are used for comparison with the data in Fig. 1. The models that take into account retention in the parabolic potential do not currently exist.

The construction of a model describing a 2D Fermi system for arbitrary values of the interaction parameter has long remained an unresolved problem. Such a model should include a description of the fermionic and bosonic limits, and also the intermediate region of strong interactions. For 3D systems, the approach based on the self-consistent mean field of the Cooper pairs turned out successful [14, 21, 39]. This approach made it possible to qualitatively correctly calculate the thermodynamic quantities at $T = 0$. After taking into account the order parameter fluctuations, it also was possible to obtain a quantitative agreement with the experiment, including the bosonic regime [40, 41]. For a 2D system, the mean-field approach [42] gives a qualitative error in the calculation of many-particle quantities, for example, the pressure, which, in the model framework, remains equal to the Fermi pressure even in the Bose limit.

A qualitatively correct description of the crossover for 2D systems has appeared only in recent years. The first such calculation was performed by the Monte Carlo diffusion method [35] for the ground state; the calculation result is shown in Fig. 1. In subsequent years, Monte Carlo methods have been significantly developed. Thus, in the Monte Carlo method with auxiliary fields [36], it turned out possible to abandon the fixed-node approximation previously used in [35]. The fixed-node approximation can lead to errors that are hard to predict [36]. In addition, the original diffusion Monte Carlo method was also developed: The scheme for optimising the variational parameters was improved, and a smooth potential of the two-particle interaction was used instead of the square well [43]. The results of this improved calculation turned out to be almost identical to the values obtained by the Monte Carlo method with auxiliary fields [36], and therefore they are not shown in Fig. 1. Both diffusion methods [35, 43] are variational, and thus, the lower pressure values correspond to a more correct model. Also, in addition to calculating the ground state, a Monte Carlo method for the final temperature has appeared [37]. It should be noted that all Monte Carlo methods give fairly close pressure values, which can be seen in Fig. 1. Small differences appear in the region of strong interactions lying between the fermionic and bosonic limits for $a_2\sqrt{n} \sim 1$.

The ground state was also investigated in the framework of the model [33], in which a mean field of the Cooper pairs is used, and the order parameter fluctuations are taken into account. The calculation result is shown in Fig. 1 [curve (*2*)]. We note that, unlike the fully mean-field approach [42], this model gives a qualitatively correct pressure dependence on the coupling parameter $a_2\sqrt{n}$, which lies above the predictions by Monte Carlo methods and is closer to the experimental data [24] (see Fig. 1).

The system properties, including those at finite temperature, are also calculated by the self-consistent T-matrix method (the Luttinger–Ward method) [44] and within the framework of the analytical approach [45] based on the Bethe–Goldstone integral equation, which takes many-particle effects into account approximately.

In the Bose regime, the pressure and chemical potential are determined by the weak repulsion between the molecular dimers. Thus, to calculate the pressure, we can use the analytical approximation for point-type bosons [46]:

$$P_{\mathrm{B}} = -\frac{P_{\mathrm{ideal}}}{4\ln(k_{\mathrm{F}}a_{2-2})}, \tag{3}$$

where a_{2-2} is the 2D s-wave scattering length of molecules on each other. In the limit $|\varepsilon_{\mathrm{B}}| \gg \hbar\omega_z$ the pressure can be expressed via the 3D molecular scattering length a_{mol}:

$$P \simeq P_{\mathrm{B}} \simeq P_{\mathrm{ideal}}\frac{a_{\mathrm{mol}}}{l_z\sqrt{8\pi}}, \tag{4}$$

where $l_z \equiv \sqrt{\hbar/(2m\omega_z)}$. In turn, a_{mol} can be related to the atomic 3D s-wave scattering length a as $a_{\mathrm{mol}} = 0.6a$ [47–49], from which the scaling law $P/P_{\mathrm{ideal}} \propto a/l_z$ follows. For the Bose region, the normalised pressure dependence on the interaction parameter is shown in Fig. 3. The experimental data [24] and formula (4) are compared. The vertical axis direction is chosen to check the dependence of $P/P_{\mathrm{ideal}} \propto a/l_z$. It can be seen that this dependence is valid in a wide range of $a_2\sqrt{n}$ values.

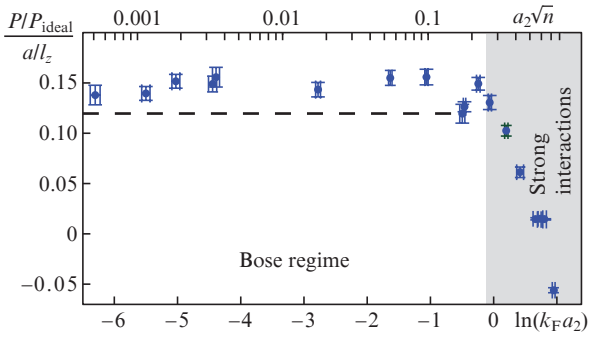

Figure 3. Testing the linear scaling for normalised pressure, $P/P_{\mathrm{ideal}} \propto a/l_z$, in the Bose crossover region. Dots show the measurement results $(P/P_{\mathrm{ideal}})/(a/l_z)$ vs. the interaction parameter [24], the dashed line is the approximation (4).

For the region of strong interactions, $a_2\sqrt{n} \sim 1$, the question of violating the two-dimensionality by interparticle interactions remains nontrivial [24, 50–52]. Even a small interaction between two atoms mixes the states of atom motion in potential (1) along the z axis. The motion of a pair of atoms remains strictly two-dimensional, since in the harmonic potential the problems of the mass centre motion and the pair interaction are separated. The contribution of three-, four- and many-particle interactions to the kinematic dimensionality requires clarification. Such a contribution is undoubtedly present in the regime of strong interaction, i.e. at the interparticle interaction energy of the order of kinetic energy. The experimental data presented in [50] evidence in favour of violating the kinematic two-dimensionality in the case of strong interatomic attraction. At the same time, these data can also be explained without the supposition on violating the kinematic two-dimensionality [52].

In conclusion, observations and modern calculations of the crossover between the Fermi-gas of atoms and Bose-gas

of molecules are in qualitative agreement with each other. Quantitatively, there are some discrepancies. First and foremost, this is the discrepancy between the data of two experiments performed with a significantly different number of particles. Also, the question of violating the kinematic two-dimensionality in the regime of strong interactions still remains open.

Acknowledgements. The work was supported by the Presidium of the Russian Academy of Sciences (Programme No. 2 'Nonlinear dynamics: fundamental problems and applications' and No. 1.4 'Actual problems of low temperature physics').

References

1. Balykin V.I., Minogin V.G., Letokhov V.S. *Rep. Progr. Phys*., **63**, 1429 (2000).
2. Onofrio R. *Phys. Usp*., **59**, 1129 (2016) [*Usp. Fiz. Nauk*, **186**, 1229 (2016)].
3. Kolachevsky N.N., Taichenachev A.V. *Quantum Electron*., **47**, 393 (2017) [*Kvantovaya Elektron*., **47**, 393 (2017)].
4. Vishnyakova G.A., Golovizin A.A., Kalganova E.S., Sorokin V.N., Sukachev D.D., Tregubov D.O., Khabarova K.Yu., Kolachevsky N.N. *Phys. Usp*., **59**, 168 (2016) [*Usp. Fiz. Nauk*, **186**, 176 (2016)].
5. Tiachenachev A.V., Yudin V.I., Bagayev S.N. *Phys. Usp*., **59**, 184 (2016) [*Usp. Fiz. Nauk*, **186**, 193 (2016)].
6. De Angelis M., Bertoldi A., Cacciapuoti L., Giorgini A., Lamporesi G., Prevedelli M., Saccorotti G., Sorrentino G., Tino G.M. *Measur. Sci. Technol*., **20**, 022001 (2009).
7. Gustavson T.L., Landragin A., Kasevich M.A. *Classic. Quantum Grav*., **17**, 2385 (2000).
8. Marti G.E., Olf R., Stamper-Kurn D.M. *Phys. Rev. A*, **91**, 013602 (2015).
9. Lim J., Lee H., Ahn J.J. *Korean Phys. Soc*., **63**, 867 (2013).
10. Sautenkov V.A., Saakyan S.A., Vilshanskaya E.V., Murashkin D.A., Zelener B.B., Zelener B.V. *Laser Phys*., **26**, 115701 (2016).
11. Ryabtsev I.I., Beterov I.I., Tretyakov D.B., Entin V.M., Yakshina E.A. *Phys. Usp*., **59**, 196 (2016) [*Usp. Fiz. Nauk*, **186**, 206 (2016)].
12. Truscott A.G., Strecker K.E., McAlexander W.I., Partridge G.B., Hulet R.G. *Science*, **291**, 2570 (2001).
13. Anderson M.H., Ensher J.R., Matthews M.R., Wieman C.E., Cornell E.A. *Science*, **269**, 198 (1995).
14. Bloch I., Dalibard J., Zwerger W. *Rev. Mod. Phys*., **80**, 885 (2008).
15. Courteille P.W., Bagnato V.S., Yukalov V.I. *Laser Phys*., **11**, 659 (2001).
16. Likhanova Yu.V., Medvedev S.B., Fedoruk M.P., Chapovsky P.L. *JETP Lett*., **103**, 403 (2016) [*Pis'ma Zh. Eksp. Teor. Fiz*., **103**, 452 (2016)].
17. Giorgini S., Pitaevskii L.P., Stringari S. *Rev. Mod. Phys*., **80**, 1215 (2008).
18. Turlapov A.V. *JETP Lett*., **95**, 96 (2012) [*Pis'ma Zh. Eksp. Teor. Fiz*., **95**, 104 (2012)].
19. Chin C., Grimm R., Julienne P., Tiesinga E. *Rev. Mod. Phys*., **82**, 1225 (2010).
20. Keldysh L.V., Kozlov A.N. *Sov. Phys. JETP*, **27**, 521 (1968) [*Zh. Eksp. Teor. Fiz*., **54**, 978 (1968)].
21. Eagles D.M. *Phys. Rev*., **186**, 456 (1969).
22. Kerbikov B.O. *Phys. At. Nucl*., **65**, 1918 (2002).
23. Bartenstein M., Altmeyer A., Riedl S., Jochim S., Chin C., Denschlag J.H., Grimm R. *Phys. Rev. Lett*., **92**, 120401 (2004).
24. Makhalov V., Martiyanov K., Turlapov A. *Phys. Rev. Lett*., **112**, 045301 (2014).
25. Loktev V.M., Quick R.M., Sharapov S.G. *Phys. Rep*., **349**, 1 (2001).
26. Korshunov S.E. *Phys. Usp*., **49**, 225 (2006) [*Usp. Fiz. Nauk*, **176**, 233 (2006)].
27. Ando T., Fowler A.B., Stern F. *Rev. Mod. Phys*., **54**, 437 (1982).
28. Kopaev Yu.V., Belyavsky V.I., Kapaev V.V. *Phys. Usp*., **51**, 191 (2008) [*Usp. Fiz. Nauk*, **178**, 202 (2008)].
29. Kagan M.Yu. *Phys. Usp*., **37**, 69 (1994) [*Usp. Fiz. Nauk*, **164**, 77 (1994)].
30. Pons J.A., Vigano D., Rea N. *Nature Phys*., **9**, 431 (2013).
31. Ong W., Cheng C., Arakelyan I., Thomas J.E. *Phys. Rev. Lett*., **114**, 110403 (2015).
32. Boettcher I., Bayha L., Kedar D., Murthy P.A., Neidig M., Ries M.G., Wenz A.N., Zurn G., Jochim S., Enss T. *Phys. Rev. Lett*., **116**, 045303 (2016).
33. He L., Lu H., Cao G., Hu H., Liu X.-J. *Phys. Rev. A*, **92**, 023620 (2015).
34. Engelbrecht J.R., Randeria M., Zhang L. *Phys. Rev. B*, **45**, 10135 (1992).
35. Bertaina G., Giorgini S. *Phys. Rev. Lett*., **106**, 110403 (2011).
36. Shi H., Chiesa S., Zhang S. *Phys. Rev. A*, **92**, 033603 (2015).
37. Anderson E.R., Drut J.E. *Phys. Rev. Lett*., **115**, 115301 (2015).
38. Petrov D.S., Baranov M.A., Shlyapnikov G.V. *Phys. Rev. A*, **67**, 031601 (2003).
39. Combescot R., Leyronas X., Kagan M.Y. *Phys. Rev. A*, **73**, 023618 (2006).
40. Hu H., Liu X.-J., Drummond P.D. *Europhys. Lett*., **74**, 574 (2006).
41. Diener R.B., Sensarma R., Randeria M. *Phys. Rev. A*, **77**, 023626 (2008).
42. Randeria M., Duan J.-M., Shieh L.-Y. *Phys. Rev. Lett*., **62**, 981 (1989).
43. Galea A., Dawkins H., Gandolfi S., Gezerlis A. *Phys. Rev. A*, **93**, 023602 (2016).
44. Bauer M., Parish M.M., Enss T. *Phys. Rev. Lett*., **112**, 135302 (2014).
45. Klawunn M. *Phys. Lett. A*, **380**, 2650 (2016).
46. Schick M. *Phys. Rev. A*, **3**, 1067 (1971).
47. Petrov D.S., Salomon C., Shlyapnikov G.V. *Phys. Rev. Lett*., **93**, 090404 (2004).
48. Brodsky I.V., Klaptsov A.V., Kagan M.Yu., Combescot R., Leyronas X. J*ETP Lett*., **83**, 273 (2005) [*Pis'ma Zh. Eksp. Teor. Fiz.*, **82**, 306 (2005)].
49. Brodsky I.V., Kagan M.Y., Klaptsov A.V., Combescot R., Leyronas X. *Phys. Rev. A*, **73**, 032724 (2006).
50. Dyke P., Fenech K., Peppler T., Lingham M.G., Hoinka S., Zhang W., Peng S.-G., Mulkerin B., Hu H., Liu X.-J., Vale C.J. *Phys. Rev. A*, **93**, 011603 (2016).
51. Martiyanov K., Barmashova T., Makhalov V., Turlapov A. *Phys. Rev. A*, **93**, 063622 (2016).
52. Turlapov A.V., Kagan M.Y. *J. Phys.: Cond. Matt*., **29**, 383004 (2017).